GEOPHYSICAL RESEARCH LETTERS, VOL. 28, NO. 22, PAGES 4215-4218, NOVEMBER 15, 2001

Dynamical response of equatorial Indian Ocean to intraseasonal winds: zonal flow

Weiqing Han,[1] David M. Lawrence,[2] and Peter J. Webster[1]

Abstract. Nonlinear and linear $4\frac{1}{2}$-layer ocean models are used to explore the dynamics of intraseasonal (20–90 day periods) zonal flow in the equatorial Indian Ocean. The model simulations suggest that the observed 40–60 day zonal surface current is forced primarily by wind associated with the Madden-Julian Oscillation (MJO), which peaks at 40–60 days. The strongest spectral peak of zonal flow, however, occurs at 90-day period in the model and a corresponding 90-day peak appears in the observed sea level data. The 90-day current results from the preferential excitation of Kelvin and Rossby waves by the lower-frequency component of intraseasonal wind and from the enhancement by Rossby waves reflected from the eastern ocean boundary.

1. Introduction

Moored current meter data in the western equatorial Indian Ocean (47°–62°E) during April 1979–June 1980 showed a spectral peak near 50 days in zonal currents at 200 m depth [*Luyten and Roemmich*, 1982]. *McPhaden* [1982] analyzed weekly data during January 1973–May 1975 in the central Indian Ocean (73°10′E, 0°41′S) and found that zonal wind is highly coherent with zonal currents down to 100 m depth at periods of 30–60 days. Measurements of current meter moorings deployed at (80°30′E, 0°45′S–5°N) during July 1993–September 1994 showed a spectral peak of zonal flow at 40–60 days near the surface [*Reppin et al.*, 1999]. Further to the east (90°E), a near 50-day oscillation of zonal surface current was observed during the Joint Air-Sea Monsoon Interaction Experiment (JASMINE) of spring 1999 [*Webster et al.*, 2001].

Modeling effort of *Moore and McCreary* [1990] suggested that the 40–50 day zonal current in the western equatorial Indian Ocean was forced by the zonal wind in the western basin. *Sengupta et al.* [2001] concluded that the 30–50 day oscillations of surface currents near central equatorial Indian Ocean from their OGCM solution result from oceanic instabilities. *Loschnigg and Webster* [2000] showed a significant intraseasonal (20–90 days) cross-equatorial oceanic heat flux in their model, suggesting that intraseasonal variability was a critical component of the annual heat balance in the Indian Ocean. *Kessler et al.* [1995] analyzed data from the western Pacific Ocean and found that zonal winds peaked at 30–60 days, whereas zonal currents peaked at 60–75 days. They suggested that this skew of frequencies might result from the selective excitation of larger-scale oceanic Kelvin waves by the lower-frequency component of the Madden-Julian Oscillation (MJO) [*Madden and Julian*, 1971]. *Hendon et al.* [1998] argued that although Kelvin waves have preferential responses at lower frequencies, they did not produce a peak at 70 days for nonpropagating wind. The 70-day peak of zonal flow resulted from the amplified response of Kelvin waves to the eastward *propagation* of wind associated with the MJO.

The importance of MJO-induced intraseasonal currents in affecting the sea surface temperature (SST) and therefore influencing the El Niño–Southern Oscillation (ENSO) in the Pacific Ocean has been capturing attention [*Johnson and McPhaden,* 1993; *Kessler et al.*, 1995; *Feng et al.*, 2000]. In the Indian Ocean, however, how currents respond to the intraseasonal atmospheric forcing is not well understood. How the currents impact the SST and therefore feedback to the atmosphere to influence the MJO and affect the Indian Ocean Dipole Mode is not known. Given that many MJOs appear first in the equatorial Indian Ocean and propagate to the western Pacific, understanding how the Indian Ocean responds and feedbacks to the atmosphere to influence the MJO will also contribute to the ENSO prediction. As an important step toward understanding the role played by the intraseasonal variabilities in the coupled ocean/atmosphere system, this paper focuses on investigating how and why the equatorial Indian Ocean zonal flow responds to the 20–90 day winds.

2. The ocean models

A nonlinear, $4\frac{1}{2}$-layer reduced gravity ocean model with active thermodynamics and mixed-layer physics is used. The four layers correspond to the surface mixed layer, seasonal thermocline, thermocline, and upper-intermediate water, respectively. Zonal velocities for layers 1–4 are u_1, u_2, u_3, and u_4. To help understand wave dynamics, a linear version of the model is also used. The linear model is dynamical and wind driven. Both models were described in greater detail by *Han et al.* [1999].

Solutions are found in a realistic Indian Ocean basin north of 29°S on a grid of dimension 55×55 km. The models are forced by 5-day mean NCEP/NCAR (National Center for Environmental Prediction/National Center for Atmospheric Research) reanalysis for the period 1980–1999. To isolate effect of wind associated with the MJO, we apply a frequency–wavenumber bandpass filter to both the zonal and meridional windstress. The filtered windstress retains the power for period 20–120 day and global zonal wavenumber 1–5, which contains primarily the MJO signal.

3. Comparison with observations

Figure 1 shows variance spectra of zonal currents from the nonlinear solution calculated from the 20-year run. The

[1]Program in Atmospheric and Oceanic Sciences, University of Colorado, Boulder, Colorado, USA
[2]Department of Meteorology, University of Reading, Reading, UK

Paper number 2001GL013701.
0094-8276/01/2001GL013701$05.00

spectra shown are ensemble averages of 10 individual spectra calculated from 730-day time series. To enable comparison with the observations described in section 1, the spectra are calculated at the western, central, and eastern equatorial Indian Ocean. Consistent with observations, broad 40–60 day spectral peaks appear in the western ocean thermocline and the central and eastern ocean surface layer. Interestingly, the strongest peaks at intraseasonal time scales occur near 90 days at all three locations. Both the 40–60 day and 90-day peaks exceed the 95% significance curves.

The 90-day oscillation has yet been detected by the current observations. The 90-day spectral peak does, however, appear in the daily sea level station data (http://ilikai.soest.hawaii.edu) near Gan island (Figure 2a), and in the TOPEX/Poseidon satellite altimeter data (2b; http://www.csr.utexas.edu) especially in the central-eastern basin where the 90-day current is strongest in the model (2c). [Note that zero values at 73°–74°E are due to representation of the Maldives in the model.] A closer comparison with the measurements of *Luyten and Roemmich* [1982] and *Reppin et al.* [1999] shows that spectral analysis of zonal flow from the model corresponding to the years and locations of these observations also exhibits the 40–60 day but not the 90-day peak (not shown). During 1999, however, zonal current spectra show both a 50-day and a 90-day peak. The former agrees with the 50-day oscillation detected by JASMINE but the latter can not be resolved by the short period of JASMINE data. The good model/data agreement suggests that the 90-day oscillation might be non-stationary in time and the short duration of the available current observations might preclude the identification of the 90-day current.

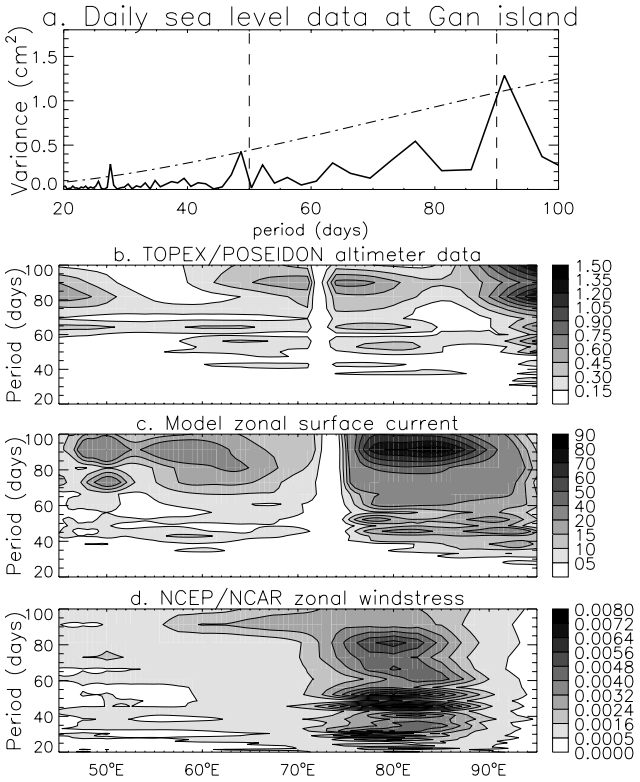

Figure 2. Variance spectra for daily sea level station data at Gan (73°09′E, 0°41′S) during 1992–1999 with dash-dotted curve representing 95% significance level (a), variance spectra along the equator for TOPEX/Poseidon satellite altimeter data (cm^2) with a 10-day resolution during 1993–1999 (b), for zonal surface current (cm^{2}s^{-2}) from the nonlinear solution during 1980–1999 (c), and for NCEP/NCAR zonal windstress (dyn^{2}cm^{-4}) during 1980–1999 (d) for the periods of 20–100 days.

4. Dynamics

To understand the relative importance of intraseasonal wind versus oceanic instabilities in generating intraseasonal zonal flow, we force the nonlinear model by winds with periods shorter than 90 days filtered out. Intraseasonal zonal current from this run exhibits very low variance, suggesting that intraseasonal zonal flow results primarily from direct wind forcing. In the central equatorial basin, however, the 40–60 day current still shows approximately one-fifth of the variance seen in Figure 1. This remanent variance may result from oceanic instabilities, as suggested by *Sengupta et al.* [2001].

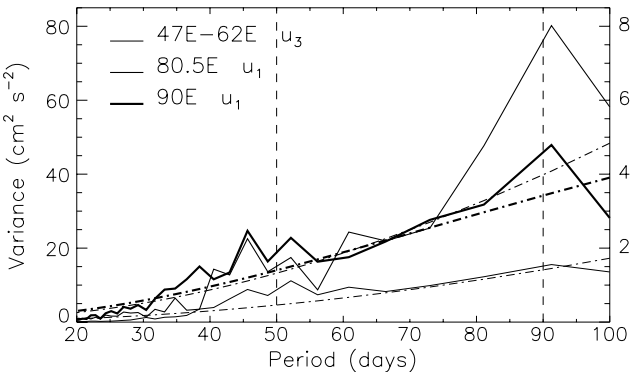

Figure 1. Variance spectra for zonal currents from the nonlinear solution in the equatorial Indian Ocean: for the western ocean (averaged over 47°E-62°E) thermocline current (u_3; thin-solid curve) and for the central (80.5°E) and eastern (90°E) ocean surface current (u_1; medium- and thick-solid curves). Vertical scales on the left are for the variance of u_1 and those on the right are for variance of u_3. The 95% significance curves are shown by dash-dotted curves.

In contrast to the zonal surface current which peaks at 90 days, zonal windstress τ^x peaks at 40–55 days with minor peaks at 35 and 80 days (Figure 2d). The skew of peak frequencies between wind and current suggests that the equatorial Indian Ocean selectively responds to the 90-day wind.

Two major processes that determine the wind-driven, intraseasonal zonal flow are assessed: directly forced response and waves reflected from the eastern ocean boundary. In addition, the impact of the eastward propagation of wind with the speed of the MJO is also evaluated. First, two solutions to the linear model, one with and the other without a damper in the eastern equatorial ocean, are obtained to isolate the impact of directly forced response from that of reflected waves [*Han et al.*, 1999]. The damped solution represents the "forced" response that is independent of reflected waves. Subtracting the results of the damped solution from the undamped (total) solution yields the effect of Rossby waves reflected from the eastern boundary, which we refer to as the "reflected wave" response. Figure 3 (top) shows variance spectra of zonal flow from the linear solution. Comparison to Figure 1 reveals that the strongest peak for the linear solution also appears near 90-day period with a

secondary peak at 40–60 days. The agreement between the linear and nonlinear solutions suggests that the wind-driven intraseasonal zonal flow is determined primarily by linear dynamics. Nonlinearities of the system tend to reduce the current amplitudes. Also shown in this figure are the variance spectra of the forced response. Variance of the forced response generally increases with the increase of period, and it is almost identical to the total solution at periods shorter than 40 days and is close to the total solution at periods of 40–55 days, suggesting that the higher frequency zonal flow results primarily from the forced response. Significant differences between the total solution and the forced response, however, exist especially near the 90-day period.

To understand why the forced response increases with increasing period and why reflected waves have a maximum effect near the 90-day period, we performed a series of idealized runs with the linear model. The model is forced by a stationary, idealized zonal wind patch that has the same amplitude and spatial structure for all the runs but oscillates at a series of periods varying from 30 to 100 days with a 5-day interval. The wind patch is centered at 80°E on the equator with an amplitude of 0.1 dyn cm^{-2} and decreases as a cosine function to zero at 60°E, 100°E, 5°N, and 5°S, resembling the realistic amplitude and scale of the zonal windstress at periods of 30–60 days. The bottom panel of Figure 3 shows the variances of zonal currents obtained from the series of solutions for both the total and forced response. The forced response increases monotonically from 30- to 85-day period and then remains almost constant from 85 to 100 days. This

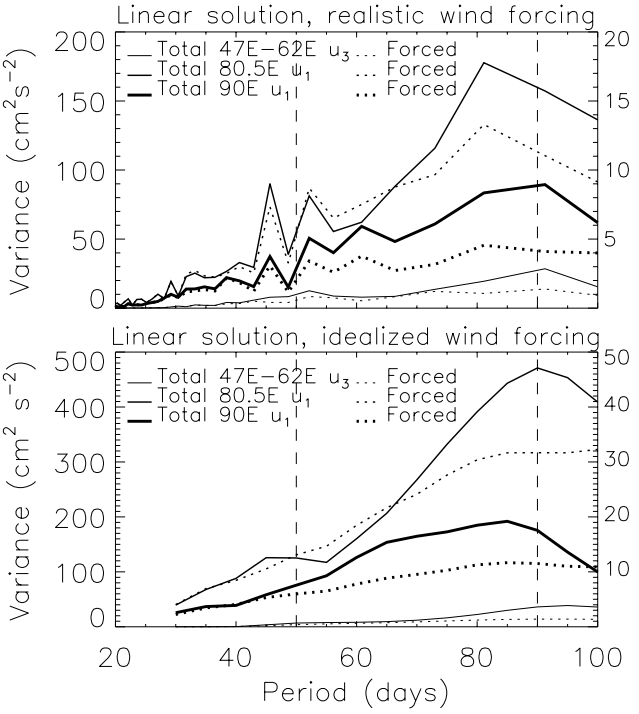

Figure 3. Variance spectra for zonal currents from the linear solutions (top): total solution (undamped, solid curves) and forced response (damped; dashed curves) for u_3 in the western ocean (thin curves) and u_1 in the central and eastern basin (medium and thick curves). Vertical scales on the left are for the variance of u_1 and those on the right are for variance of u_3. (bottom) Same as top except for the linear solution forced by the idealized, stationary wind.

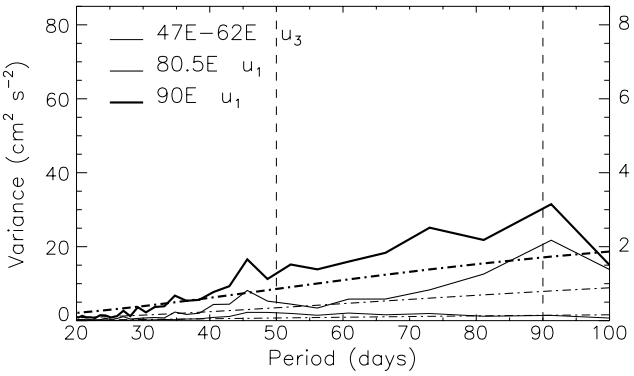

Figure 4. Same as Figure 1 except for the MJO wind forcing.

behavior results primarily from the preferential excitation of combined Rossby and Kelvin waves near 80–85 day period, and from the monotonically increasing local response due to longer acceleration time at longer periods. Amplitudes of Kelvin and Rossby waves are proportional to the zonal integral of $[X(x)e^{-ikx}]$, where $X(x)$ is the zonal structure of τ^x and k is the wavenumber for Kelvin or Rossby waves. For the given wind scale, response of the combined Kelvin and Rossby waves reaches a relative maximum at 80–85 day period, similar to the discussion of *Kessler et al.*, [1995] except that Rossby waves are also involved here.

Reflected Rossby waves, which have not been discussed in the Pacific Ocean, tend to enhance the forced response especially near the 90-day period because of the near resonance response of the second baroclinic mode (the gravest mode in the Indian Ocean; see *Moore and McCreary*, [1990]; *Han et al.*, [1999]) with the 90-day wind. Let T be the forcing period, L be the basin width, and c be the Kelvin-wave speed of a baroclinic mode. Then, the response is resonant when $T=\frac{4L}{mc}$, where m is a positive integer. In the equatorial Indian Ocean, the second baroclinic mode with $c = 165$ cm s^{-1} is near resonant with the 90-day wind when m=2 and 180-day wind when m=1 [see *Han et al.*, 1999].

Finally, to test the impact of eastward propagation of wind, we force the linear model with the earlier-described idealized winds but move eastward at a speed of 2, 3, 4, and 5 m s^{-1}, respectively, typical speeds of the MJO in the Indian Ocean [*Hendon et al.*, 1998]. In these experiments, the spectral peaks weaken in the central and western ocean but strengthen in the eastern basin, because the eastward movement of wind weakens the westward radiating Rossby waves and strengthens the eastward propagating Kelvin waves, as discussed by *Tang and Weisberg* [1984].

5. Forcing by the MJO

To understand how much the wind associated with the MJO, the dominant mode of intraseasonal variability (ISV) in the tropical troposphere that couples with convection, accounts for the intraseasonal current, we force the nonlinear model by windstress with the MJO signal (see section 2) removed. Current difference between the solutions with and without the MJO signal estimates the MJO impact. Figure 4 shows variance spectra of zonal current forced by the MJO wind. Comparison with Figure 1 reveals that the MJO has a maximum influence in the eastern basin (90°E), where it explains 68% of the total variance at 90 days and

60% at 45 days. Near the central ocean (80.5°E), impact of the MJO decreases but still explains 40% of the variance at 45-day and 25% at 90-day period. Consequently, the 40–60 day currents observed by *Reppin et al.* [1999] and *Webster et al.* [2001] result largely from the MJO wind forcing. In the western ocean thermocline, however, the intraseasonal zonal flow is not likely forced by the MJO. This westward decreasing effect of the MJO results predominantly from the weakened westward radiating Rossby waves and strengthened eastward propagating Kelvin waves due to the eastward propagation of the MJO.

This result is particularly interesting because it may imply air-sea coupling at the 90-day period that can explain the across basin scale (Figure 2) and equatorially trapped 90-day wind. Initially, the equatorial Indian Ocean has a selective response to the 90-day wind associated with the MJO, producing a 90-day peak in the surface current (Figure 4). This current advects the mean SST gradient, causing a 90-day SST variability that feedbacks to the atmosphere to enhance the MJO associated lower-frequency wind and excite other types of ISVs, such as the convectively coupled westward propagating Rossby waves and eastward propagating Kelvin waves [*Wheeler and Kiladis*, 1999] or waves that are not coupled with convection, therefore producing the across basin scale wind at 90 days. The strengthened 90-day wind feedbacks to the ocean to enhance the 90-day current (Figure 1). This coupled process, however, might be possible only during years when the MJO associated 90-day wind is strong enough to produce a significant SST variability. In fact, similar process may have occurred in the Pacific Ocean, where the ocean has a peak response near 70-day period and a corresponding 70-day spectral peak occurs in the NCEP daily zonal wind across the Pacific basin (not shown).

6. Summary and discussion

Modeling results presented here suggest that the observed 40–60 day zonal surface current in the equatorial Indian Ocean is primarily forced by the 40–60 day zonal wind associated with the MJO. In the western ocean thermocline, however, the 40–60 day current is driven by wind associated with the ISVs other than the MJO. The strongest spectral peak of intraseasonal zonal flow occurs near 90-day period in our solutions, and the 90-day peak appears in the sea level data. The peak of 90-day current results from the preferential excitation of Kelvin and Rossby waves by the lower-frequency component of intraseasonal wind in conjunction with the enhancement by Rossby waves reflected from the eastern boundary. The across basin scale and equatorially trapped zonal wind near 90-day period in the Indian and 70-day period in the Pacific Ocean coincides with the peak oceanic response in the two oceans, implicating the potential air-sea interaction at these periods.

Acknowledgments. We thank Dr. J.P. McCreary for his helpful suggestions and NCEP/NCAR for providing the forcing fields at http://www.cdc.noaa.gov. The authors were supported by NSF grant ATM-9526030.

References

Feng, M., R. Lukas, P. Hacker, R. Weller, and S. Anderson, Upper-ocean heat and salt balances in the western equatorial Pacific in response to the intraseasonal oscillation during TOGA COARE, *J. Climate, 13*, 2409–2427, 2000.

Han, W., J.P. McCreary, D.L.T. Anderson, and A.J. Mariano, Dynamics of the eastward surface jets in the equatorial Indian Ocean, *J. Phys. Oceanogr., 29*, 2191-2209, 1999.

Hendon, H.H., B. Liebmann, and J.D. Glick, Oceanic Kelvin waves and the Madden-Julian oscillation, *J. Atmos. Sci., 55*, 88–101, 1998.

Johnson, E.S. and M.J. McPhaden, Structure of intraseasonal Kelvin waves in the equatorial Pacific Ocean, *J. Phys. Oceanogr., 23*, 608–625, 1993.

Kessler, W.S., M.J. McPhaden, and K.M. Weickmann, Forcing of intraseasonal Kelvin waves in the equatorial Pacific, *J. Geophys. Res., 100*, 10613–10631, 1995.

Loschnigg, J. and P.J. Webster, A coupled ocean-atmosphere system of SST modulation for the Indian Ocean, *J. Climate, 13*, 3342–3360, 2000.

Luyten, J.R and D. Roemmich, Equatorial currents at semiannual period in the Indian Ocean, *J. Phys. Oceanogr., 12*, 406–413, 1982.

Madden, R.A. and P.R. Julian, Detection of a 40–50 day oscillation in the zonal wind of the tropical Pacific, *J. Atmos. Sci., 28*, 702–708, 1971.

McPhaden, M.J., Variability in the central equatorial Indian Ocean. Part 1: Ocean dynamics, *J. Mar. Res., 40*, 157–176, 1982.

Moore, D.W. and J.P. McCreary, Excitation of intermediate-frequency equatorial waves at a western ocean boundary: with application to observations from the Indian Ocean, *J. Geophys. Res., 95*, 5219–5231, 1990.

Reppin, J., F.A. Schott, J. Fischer, and D. Quadfasel, Equatorial currents and transports in the upper central Indian Ocean: Annual cycle and interannual variability, *J. Geophys. Res., 104*, 15,495–15,514, 1999.

Sengupta, D., R. Senan, and B.N. Goswami, Origin of intraseasonal variability of circulation in the tropical central Indian Ocean, *Geophys. Res. Lett., 28*, 1267–1270, 2001.

Tang, T.Y. and R.H. Weisberg, On the equatorial Pacific response to the 1982/1983 El Niño–Southern Oscillation event, *J. Mar. Res., 42*, 809–829, 1984.

Webster, P.J., E.F. Bradley, C.E. Fairall, J.S. Godfrey, P. Hacker, R. Lukas, Y. Serra, R.A. Houze Jr., J.M. Humman, D.M. Lawrence, C.A. Russell, M.N. Ryan, K. Sahami, P. Zuidema, The Joint Air-Sea Monsoon Interaction Experiment (JASMINE): (2) Results from the field phase, submitted to *Bull. Amer. Meteor. Soc.*, 2001.

Wheeler, M. and G.N. Kiladis, Convectively coupled equatorial waves: analysis of clouds and temperature in the wavenumber-frequency domain, *J. Atmos. Sci., 56*, 374–399, 1999.

W. Han and P. Webster, Program in Atmospheric and Oceanic Sciences, University of Colorado, Boulder, Colorado, USA. (whan@monsoon.colorado.edu)

D. Lawrence, Department of Meteorology, University of Reading, Reading, UK. (dml@met.reading.ac.uk)

(Received June 28, 2001; revised August 26, 2001;
accepted September 14, 2001.)